

Fine-Tuning Visual Autoregressive Models for Subject-Driven Generation

Jiwoo Chung, Sangeek Hyun, Hyunjun Kim, Eunseo Koh, MinKyu Lee, Jae-Pil Heo*
 Sungkyunkwan University

{jiwoo.jg, hse1032, arithu3, rainniee999, 2minkyulee, jaepilheo}@gmail.com



Figure 1. Our method achieves high subject fidelity and text alignment in subject-driven generation through Visual autoregressive models.

Abstract

Recent advances in text-to-image generative models have enabled numerous practical applications, including subject-driven generation, which fine-tunes pretrained models to capture subject semantics from only a few examples. While diffusion-based models produce high-quality images, their extensive denoising steps result in significant computational overhead, limiting real-world applicability. Visual autoregressive (VAR) models, which predict next-scale tokens rather than spatially adjacent ones, offer significantly faster inference suitable for practical deployment. In this paper, we propose the first VAR-based approach for subject-driven generation. However, naïve fine-tuning VAR leads to computational overhead, language drift, and reduced diversity. To address these challenges, we introduce selective layer tuning to reduce complexity and prior distillation to mitigate language drift. Additionally, we found that the early stages have a greater influence on the generation of subject than the latter stages, which merely synthesize minor details. Based on this finding, we propose

scale-wise weighted tuning, which prioritizes coarser resolutions for promoting the model to focus on the subject-relevant information instead of local details. Extensive experiments validate that our method significantly outperforms diffusion-based baselines across various metrics and demonstrates its practical usage. Codes are available at github.com/jiwoogit/ARBooth.

1. Introduction

With recent advances in text-to-image (T2I) generative models [28, 41, 44, 47, 67], numerous real-world applications [1, 4, 7, 8, 19, 20, 33, 48, 69] have emerged and gained widespread adoption. Among these applications, subject-driven generation (also called text-to-image personalization) [13, 40, 48, 53] represents the content of target subject using unique text embedding by optimizing the parameters or embeddings with only a few examples.

Most existing methods for subject-driven generation rely on pretrained diffusion models [41, 47], leveraging their ability to produce diverse and visually plausible images. However, the diffusion process inherently requires a large

* Corresponding author

number of denoising steps (e.g., 50 DDIM steps) [55], incurring significant computational cost. This inefficiency limits the applicability of diffusion-based methods in real-world scenarios, where fast inference and computational efficiency is crucial.

Recently, a novel family of generative models called Visual autoregressive (VAR) [58] has been introduced. Unlike a typical autoregressive model that first encode image into tokens and sequentially predicts tokens in a raster scan order, it reformulates autoregressive modeling to predict next-scale tokens at once, instead of different locations. This approach significantly accelerates inference speeds—approximately 20 times faster than diffusion models—while achieving state-of-the-art performance in image quality, data efficiency, and scalability [58]. Notably, recent work [18] further demonstrated VAR’s scalability in large-scale T2I generation tasks. Despite these promising advantages, the application of VAR models to subject-driven generation remains unexplored.

In this paper, we present the first investigation of subject-driven generation within the VAR framework. Drawing inspiration from diffusion-based approaches [26, 48], we initially explore fine-tuning both model parameters and textual embeddings to capture the target subject. However, naïve fine-tuning presents challenges such as computational inefficiency, language drift, and reduced diversity, which have also been identified in language models [31, 38] and diffusion-based approaches [11, 26, 48].

To effectively address these issues, we introduce selective layer tuning and prior distillation. Through our analysis, we observe that cross-attention and feed-forward layers in the VAR transformer exhibit larger weight updates. As larger updates imply the significance of weights to capture the subject-relevant information [26, 35], we selectively fine-tune the module mostly updated. This approach substantially reduces computational overhead without sacrificing performance. Additionally, our proposed prior distillation leverages the pretrained model’s semantic knowledge to produce diverse instances of the same subject class without requiring extensive external datasets. By utilizing the efficient inference of the VAR architecture, our approach enables end-to-end fine-tuning, effectively mitigating language drift and improving output diversity.

Furthermore, we analyze the generation impact of different scales in the VAR architecture. Specifically, we observe that coarser-scale token maps have a greater influence on synthesizing the identity of subject, whereas finer-scale tokens have a relatively smaller impact. Motivated by this observation, we propose scale-wise weighted tuning, which prioritizes coarser resolutions to effectively capture subject semantics while placing less emphasis on minor variations such as finer-scale details. Extensive experiments demonstrate that our method accurately encodes the target concept

while maintaining robust editing capabilities, significantly outperforming diffusion-based baselines.

Our main contributions are summarized as follows:

- We introduce the first attempt for optimization-based subject-driven generation method that utilizes a large-scale pretrained VAR model.
- We propose three components based on our findings to mitigate several challenges; selective layer tuning, scale-wise weighted tuning, and prior distillation.
- Extensive experiments validate that our method significantly outperforms diffusion-based baselines in terms of subject fidelity, text alignment, and inference speed.

2. Related Work

Autoregressive visual generation. Autoregressive models (AR) for visual generation typically follow a raster scan manner [5, 46, 59]. Early methods [9, 30, 45, 61, 70] employ vector quantization (VQ) to transform image patches to discrete tokens, predicting the next token with transformer models. Building on this pipeline, numerous works [25, 57, 63, 64, 71] have scaled VQ-based transformers for advanced text-to-image and video generation tasks. Recently, Visual autoregressive (VAR) [58] models have introduced a next-scale prediction framework, significantly improving image quality. Infinity [18] incorporates bit-wise quantization [72, 74] to enable large-scale text-to-image generation within this framework for scalability. Our approach extends this paradigm by introducing VAR in subject-drive generation, effectively capturing diverse subjects through fine-tuning.

Applications in AR. Recent developments such as LlamaGen2 [56] have enhanced autoregressive generation by improving image compression, scaling architectures, and improving training procedures. Following this direction, ControlAR [36] and EditAR [39] propose methods for injecting spatial controls like edge maps or depth maps into autoregressive models. Despite VAR’s demonstrated potential, few studies have explored its application. ControlVAR [34] and Car [68] extend controllable generation to VAR frameworks using scale-wise prediction. However, subject-driven generation remains largely unexplored in VAR contexts. Our work addresses this gap by proposing novel fine-tuning strategies tailored for subject-driven tasks.

Text-to-Image subject-driven generation. Early diffusion-based approaches represent subjects through optimized textual embeddings or full-model parameter fine-tuning, such as in Textual Inversion [13] and DreamBooth [48]. Recent approaches [6, 14, 24, 26, 32, 52, 65, 66] emphasize efficient adaptations by either fine-tuning specific subsets of model parameters or introducing adapter modules; for example, CustomDiffusion [26] targets cross-attention layers. However, current methods predominantly rely on diffusion-based architectures. To our knowledge, we

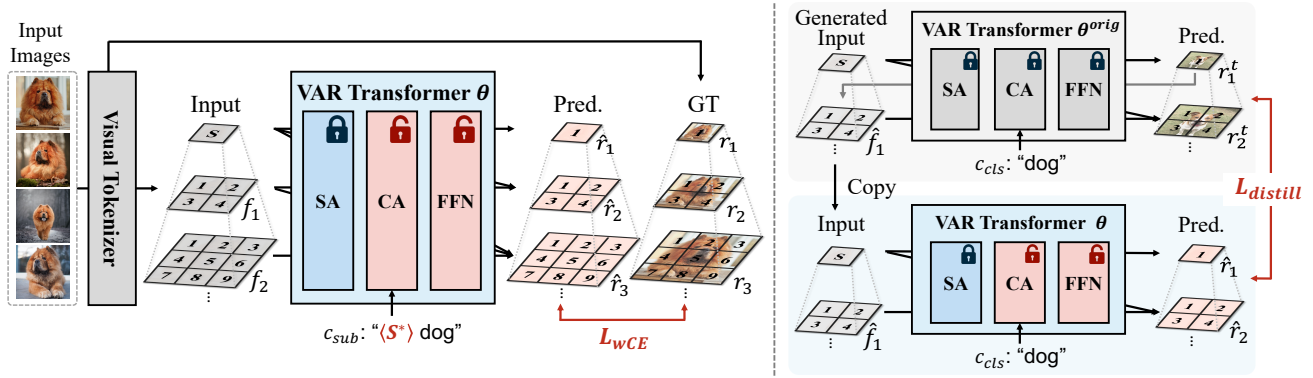


Figure 2. Overall Framework. (Left) Subject-Driven Fine-Tuning. We first encode the subject images into K multi-scale token maps (r_1, \dots, r_K) using a visual tokenizer. Given a randomly sampled subject image, we fine-tune VAR transformer to reconstruct the corresponding token maps ($\hat{r}_1, \dots, \hat{r}_K$) to inject the concept of subject to the generator. During the optimization, we selectively fine-tune only the cross-attention (CA) and feed-forward network (FFN) layers (Sec. 4.1). Furthermore, we introduce a scale-wise weighted cross-entropy loss (\mathcal{L}_{wCE}) to efficiently focus coarser scales that contribute significantly to capturing subject semantics (Sec. 4.2). **(Right) Prior Distillation.** To address language drift and enhance output diversity, we generate token maps using the original transformer θ^{orig} , conditioned on a class noun prompt c_{cls} (e.g., “dog”). These token maps serve as guidance for the fine-tuned transformer, where a distillation-based loss ($\mathcal{L}_{\text{distill}}$) helps preserve the pretrained model’s semantic prior (Sec. 4.3). Finally, we jointly optimize the CA and FFN layers using both losses ($\mathcal{L}_{wCE}, \mathcal{L}_{\text{distill}}$) to maintain subject fidelity and generative consistency.

propose the first exploration of subject-driven text-to-image personalization in large-scale autoregressive models.

Moreover, our analysis also provide valuable insights for future VAR research. For example, we find that FFN layers in VAR are crucial, which aligns closely with recent observation in language models [15, 16]. We expect that these insights can serve as a bridge for transferring techniques from language models to AR-based vision models.

3. Preliminary

3.1. Next-token Prediction

Traditional autoregressive (AR) models generate images by predicting tokens sequentially in a raster scan order [50, 59, 60]. Specifically, a visual autoencoder first encodes an image into a latent representation, which is then quantized into a sequence of discrete tokens $x = (x_1, x_2, \dots, x_T)$. To synthesize an image, the AR model iteratively predicts the probability distribution of the next token x_t given its preceding tokens $x_{<t} = (x_1, x_2, \dots, x_{t-1})$ and condition c :

$$p(x) = \prod_{t=1}^T p(x_t | x_{<t}, c). \quad (1)$$

After sampling tokens based on these predicted probabilities, the generated tokens are decoded into an image via the visual autoencoder.

3.2. Next-scale Prediction

Visual autoregressive (VAR) [58] models reformulate autoregressive prediction units from tokens at different spa-

tial locations to tokens at different resolutions. That is, it predicts “next-scale” tokens rather than sequential tokens. Specifically, given an image I , the visual encoder \mathcal{E} first encodes it into a feature map f . VAR then iteratively quantizes f into K multi-scale token maps $r = (r_1, r_2, \dots, r_K)$. Given previous token maps $r_{<k}$ and a condition c , the k -th scale tokens r_k are computed as:

$$f_k = f - \sum_{i=1}^{k-1} \text{upsample}(\text{Lookup}(r_i)), \quad (2)$$

$$p(r) = \prod_{k=1}^K p(r_k | r_{<k}, c), \quad (3)$$

where $\text{Lookup}(\cdot)$ is a lookup table mapping each token r_i to its closest entry in a learnable codebook, and $\text{upsample}(\cdot)$ is a bilinear upsampling operation.

Recently, the next-scale prediction framework has demonstrated its effectiveness for large-scale text-to-image generation. Infinity [18] adopts bit-wise quantization techniques [72, 74], significantly expanding the available code-word space. As a result, it achieves text fidelity and aesthetic quality comparable to state-of-the-art diffusion-based methods, while providing faster inference speed. Thus, leveraging these advantages for subject-drive generation has the potential of extending this framework.

4. Method

Given a set of n subject images $\mathcal{X} = \{I_1, I_2, \dots, I_n\}$, existing subject-driven methods typically personalize text-to-

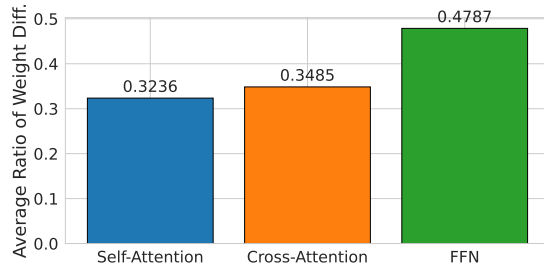


Figure 3. Average Ratio of Weight Differences. We measure the weight differences between the original model (θ^{orig}) and its fine-tuned counterpart (θ) using averaged ratios across layers. The averaged ratio is computed as $|\theta^{\text{orig}} - \theta|/(|\theta^{\text{orig}}| + \epsilon)$, where ϵ is a small constant. Notably, the feed-forward networks (FFN) exhibit significantly larger weight changes compared to other layers, indicating their importance to fine-tuning.

image (T2I) diffusion models or text embeddings c_{sub} (e.g., $\langle S^* \rangle$ dog) for represent specific subject semantics. During inference, these fine-tuned models generate images aligned with context prompts (e.g., $\langle S^* \rangle$ dog in the desert). Despite their successes, diffusion-based approaches are limited in practical applications thanks to slow inference speeds arising from extensive denoising steps. Recently, visual autoregressive (VAR) models have been introduced as a promising solution due to their significantly faster inference capability. We therefore aim to address subject-driven generation by harnessing the generative capabilities of a pretrained large-scale T2I VAR model. However, naïve fine-tuning still brings several challenges, such as computational overhead, language drift, and reduced diversity. In this paper, we address these issues through novel techniques based on our comprehensive analysis.

4.1. Selective Layer Tuning

One straightforward approach for subject-driven generation is fine-tuning all layers of the generator with additional subject-specific text embeddings [48]. However, excessive tuning of all layers increases computational cost and can degrade generated image quality due to overfitting, potentially harming the model’s original generative capabilities.

To address this, we aim to identify a compact yet effective subset of parameters for fine-tuning, inspired by previous works [26, 35]. Specifically, we analyze layer-wise adaptation during personalization by measuring weight changes between the original and fully fine-tuned VAR models. As reported in Fig. 3, feed-forward layers exhibit the most significant weight changes. This suggests that these layers primarily integrate subject-specific information. We first attempt to fine-tune only the feed-forward layers while keeping other layers fixed. However, we empirically observe a deterioration in text alignment, as shown in Fig. 7. To ensure alignment with the target text and subject,

we therefore selectively fine-tune only these two components, effectively capturing the subject concept while preserving overall generative capability.

4.2. Scale-wise Weighted Tuning

Prior studies on diffusion models have revealed that their generative capability varies across different timesteps, with the distance between two timesteps in the diffusion process decreasing over timesteps [75, 76]. Leveraging these observations, these methods prioritize training at earlier timesteps, where the models show significant updates, thus improving both efficiency and generation quality [75, 76].

Similar to diffusion models, the VAR framework synthesizes images in a coarse-to-fine manner using a multi-scale residual quantization method. Consequently, its generative capability varies across different resolutions. To specify this, we analyze the contribution of each scale in image generation. After identifying that each scale contributes differently to generation, we fine-tune the model at a scale-wise level to efficiently adapt to the subject concept.

Specifically, we first encode a given image I and a noise image \mathcal{N} into multi-scale token maps (r_1, \dots, r_K) and $(r_1^{\mathcal{N}}, \dots, r_K^{\mathcal{N}})$, respectively. We then progressively construct noise-corrupted token representations by substituting finer-scale tokens from the subject image with those from the noise image $(r_1, \dots, r_k, r_{k+1}^{\mathcal{N}}, \dots, r_K^{\mathcal{N}})$. These corrupted representations are decoded to analyze their impact on the generation process. As shown in Fig. 4, we observe that coarser resolutions lead to significant changes of the generated image whereas finer resolutions induce only minor variations in VAR. This behavior aligns with diffusion models [75, 76], where the most drastic variations occur in the earlier stages. Quantitatively, we also measure the mean square error (MSE) between the reference image and its noise-corrupted counterpart across scales, indicating that VAR framework relies even more heavily on early-stage representations compared to diffusion models, as shown in Fig 5.

Inspired by this observation, we prioritize training on scales with greater contributions during subject-driven fine-tuning. In detail, we introduce a scale-wise weighted cross-entropy loss (\mathcal{L}_{wCE}) which assigns higher weights to coarse scales and lower weights to fine scales:

$$\mathcal{L}_{\text{wCE}} = - \sum_{k=1}^K w_k \log p_{\theta}(r_k \mid r_{<k}, c_{\text{sub}}), \quad (4)$$

where r_k denotes the multi-scale token map derived from subject images, and w_k represents the hyperparameter to weight for each scale, following the order $w_1 \geq w_2 \geq \dots \geq w_K$. This strategy enables the fine-tuned model to effectively capture subject-specific semantics, while preserving its original generative capabilities.

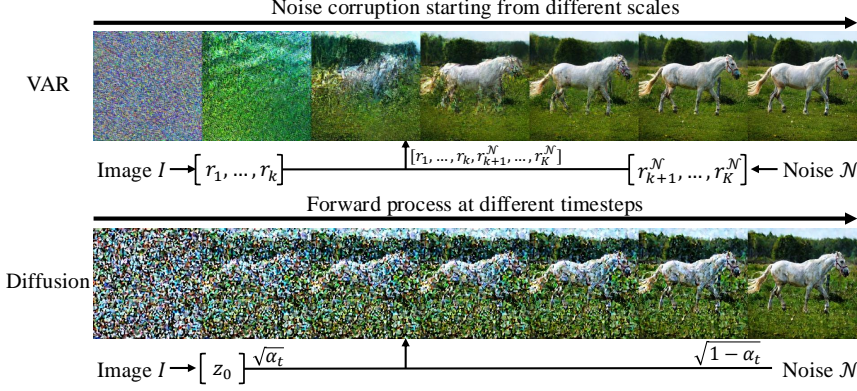


Figure 4. **Visualization of noise corruption across different stages.** (Top row) Scale-wise noise corruption in VAR. To investigate each scale’s contribution to image generation, we encode a given and noise image I and \mathcal{N} into token maps r and r^N , respectively. When synthesizing images by merging token maps from a given and noise images based on a specific scale, we observe coarser token maps contribute to the content while finer tokens adjust the local details. (Bottom row) Timestep-based forward process in diffusion model. Similar to VAR, we encode the reference image into a latent representation (z_0) [47] and visualize images at each timestep during the forward diffusion process [22, 54]. Interestingly, scales of VAR and timesteps of diffusion exhibit similar disruption patterns, implying both coarser scale and higher time step contribute the actual content, while finer scale and lower timesteps adjust the details. Experimental details are available in Sec. 4.2.

4.3. Prior Distillation

We further introduce prior distillation to address language drift and reduced diversity. Language drift, previously observed in language model fine-tuning [31, 38], occurs when a model gradually loses its pretrained knowledge, becoming overly focused on fine-tuned tasks. Similarly, we find that the fine-tuned VAR model tends to forget how to generate diverse instances within the same subject class. For example, when prompted with a generic class noun (e.g., “a dog”), the personalized model consistently generates images resembling the specific fine-tuned subject. In previous diffusion-based methods such as DreamBooth [48], language drift is mitigated by first collecting numerous same-class images and jointly fine-tuning them alongside subject-specific images. However, this approach requires substantial data collection, which is often costly and impractical.

In our autoregressive framework, we propose an end-to-end prior preserving approach called *prior distillation*. Unlike diffusion-based methods that necessitate data collection, our approach leverages the fast inference capability of VAR to generate diverse instances of the subject’s class. Specifically, the efficiency of VAR’s inference allow our distillation method to mitigate language drift without the burden of gathering large same-class datasets.

Concretely, we designate the large-scale pre-trained VAR transformer as the teacher in distillation process, as visualized in Fig. 2. Given a class prompt (c_{cls}), the original (teacher) model θ^{orig} generates multi-scale tokens.

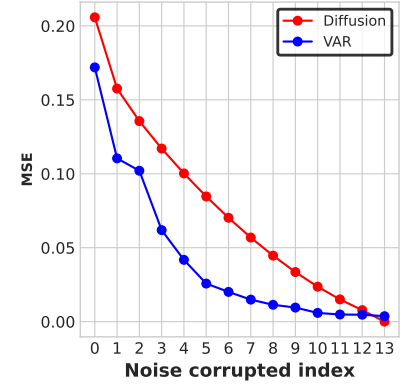


Figure 5. **MSE analysis between reference and noise-corrupted images.** We quantitatively analyze the impact of noise corruption at various scale and timesteps for VAR and diffusion models by measuring mean squared error (MSE). Both architectures show similar trends, though VAR exhibits a stronger curvature, highlighting greater sensitivity at early stages.

Instead of reconstructing images from these tokens and subsequently re-encoding them via the visual autoencoder and multi-scale quantizer, we directly utilize the original model’s token outputs to guide predictions from the fine-tuned model. This approach effectively bypasses redundant encoding-decoding steps, significantly streamlining the distillation process.

The distillation objective is defined as follows:

$$\mathcal{L}_{\text{distill}} = \sum_{k=1}^K D_{\text{KL}} \left(p_{\theta^t}(r_k^t \mid r_{<k}^t, c_{\text{cls}}) \parallel p_{\theta}(r_k \mid r_{<k}, c_{\text{cls}}) \right), \quad (5)$$

where r_k^t denotes the token maps generated by the original model and D_{KL} denotes the KL-divergence between two probabilities. Through prior distillation, we effectively regulate the model’s fine-tuning by consistently exposing the original semantic knowledge. This ensures diverse generation and mitigates language drift.

In summary, we fine-tune the CA and FFN layers of the transformer and the text embedding while jointly optimizing the scale-wise weighted cross-entropy loss (\mathcal{L}_{wCE}) and prior distillation loss ($\mathcal{L}_{\text{distill}}$) to enhance subject fidelity and preserve generative consistency.

5. Experiment

5.1. Implementation Details

We conduct all experiments using Infinity-2B model [18], pretrained on the LAION [51], COYO [2], and OpenIm-

ages [27] datasets. We follow the default configuration provided by Infinity ($K = 13$) and apply classifier-free guidance [21] to logits as our default setting. The model is fine-tuned at a resolution of 1024 for 600 iterations with a batch size of 2 and use AdamW [37] optimizer ($\beta_0 = 0.9, \beta_1 = 0.97$) with a learning rate of $6e - 3$ on a single NVIDIA A6000 GPU. Additionally, we apply random resize and center crop augmentations following [62].

5.2. Evaluation Protocol

Dataset. We utilize the dataset from ViCo [17], originally collected in previous works [13, 48, 49]. This dataset comprises 16 subject concepts (5 living and 11 non-living), each paired with 31 textual prompts. For evaluation, we generate 8 images per concept-prompt pair, resulting in a total of 3,968 generated images.

Baselines. We evaluate our proposed method against five diffusion-based state-of-the-art baselines: Textual Inversion (TI) [13], DreamBooth (DB) [48], CustomDiffusion (CD) [26], ELITE [65], ViCo [17], and Dream-Matcher (DM) [40]. For ELITE, we employ the official implementation. For TI, DB, CD, ViCo and DM, we adopt the pretrained weights or use the value provided by DM’s publicly available implementation based on Stable Diffusion (SD) 1.4 [47], following their default configuration.

Metrics. Following previous studies [13, 26, 40, 48], we evaluate both subject fidelity and text prompt fidelity. For subject fidelity, we measure image similarity between the generated images and the reference subject using DINO [3] and CLIP [43], denoted as I_{dino} and I_{clip} , respectively. For text prompt fidelity, we compute CLIP image-text similarity by comparing the visual features of the generated images with the textual features of the prompts, excluding placeholders, and denote this as T_{clip} .

For the ablation study, we measure a prior preservation metric (PRES) [48], defined as the average pairwise similarity between the DINO embeddings of generated images from random subjects of the prior class and real images of our target subject. A higher PRES value indicates that the random subjects resemble the target subject, suggesting that the model’s ability to maintain the original has broken down. Furthermore, we compute diversity (DIV) [48] using the average pairwise LPIPS [73] distance between generated images of the same subject with the same prompt. These metrics capture a crucial property by indicating whether the model fails to preserve prior knowledge.

5.3. Quantitative Comparison

As shown in Tab. 1, our method outperforms diffusion-based baselines on both I_{dino} and I_{clip} , indicating improved subject alignment. Notably, it also achieves better performance on T_{clip} , reflecting enhanced alignment with the text prompt. Although these metrics often involve a trade-off,

Model	$I_{dino} \uparrow$	$I_{clip} \uparrow$	$T_{clip} \uparrow$	Time ↓
TI [13]	0.529	0.770	0.220	18s
DB [48]	0.640	0.815	0.236	18s
ELITE [65]	0.584	0.783	0.223	11s
CD [26]	0.659	0.815	0.237	18s
ViCo [17]	0.643	0.816	0.228	15s
DM [40]	0.682	0.823	0.234	32s
Ours	0.705	0.824	0.253	0.5s

Table 1. Quantitative comparison with baselines.

Preference	CD [26]	DM [40]	Ours
Subject Fidelity \uparrow	15%	18%	67%
Prompt Alignment \uparrow	11%	10%	79%

Table 2. Subject fidelity and prompt fidelity user preference.

our method achieves higher values in both, demonstrating a strong enhancement.

In addition, we measure the inference time for generating a single image using a target prompt on an A6000 GPU, reported as the “Time” column in Tab. 1. Our method completes the inference in 0.5 seconds, whereas diffusion-based baselines take significantly longer. This speed advantage stems from a shorter progressive inference scheme processing from coarse to fine scales. In contrast, diffusion-based methods require numerous denoising steps within the same dimensional space. These results highlight the practical potential of our approach for real-world applications.

Furthermore, we compare our method with CD [26] and DM [40], which achieve the highest quantitative performance among the baselines in subject fidelity and text alignment, respectively. We conduct a user study with 20 participants, collecting a total of 640 responses from 32 comparative questions. Samples are randomly selected from the experimental dataset. Each question presents real subject images, a text prompt, and three generated images from the baseline methods. Users are asked to select the image that best preserves subject identity and prompt fidelity. As shown in Tab. 2, our method is preferred by (67%, 79%) of users over CD and DM, respectively.

5.4. Qualitative Comparison

As shown in Fig. 6, our method not only preserves the structure details of the subject image but also aligns closely with the text prompt. For example, in the second row, our approach accurately reconstructs the teddybear’s structure, whereas the baseline methods struggle to maintain structural integrity and fails to generate the water details correctly. Furthermore, in the third row, our method successfully generates a cat wearing a Santa hat or a police outfit, while the baseline methods struggle to match the clothing with the cat or fail to generate the appropriate attire.

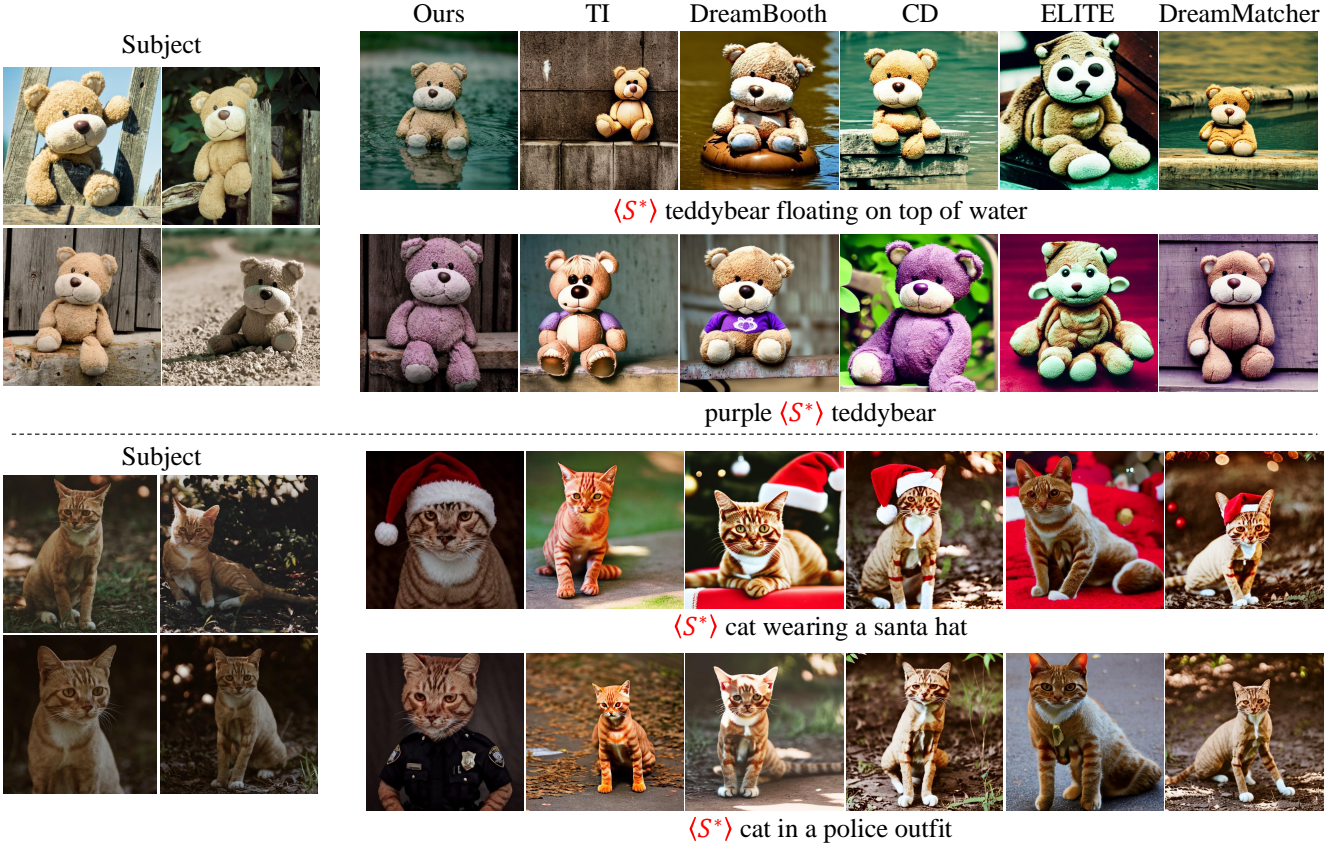


Figure 6. Qualitative comparison with diffusion-based baselines.

Variant	$I_{dino} \uparrow$	$I_{clip} \uparrow$	$T_{clip} \uparrow$	$PRES \downarrow$	$DIV \uparrow$
Sec. 4.1	Ours	0.786	0.853	0.267	0.709 0.272
	w/ Full	0.796	0.850	0.267	0.776 0.254
Sec. 4.2	Ours	0.786	0.853	0.267	0.709 0.272
	w/o SWT	0.774	0.840	0.271	0.792 0.285
Sec. 4.3	Ours	0.786	0.853	0.267	0.709 0.272
	w/o PD	0.823	0.896	0.236	0.839 0.209

Table 3. Quantitative ablation study on proposed strategies.

5.5. Ablation Study

We further analyze the influence of our proposed techniques through comprehensive ablation studies. To this end, we train ablated models on five living subject concepts using 31 prompts, generating eight samples per prompt-subject pair for a total of 1240 images.

Selective layer tuning ablation. As shown in the first row of Tab. 3, we compare our model fine-tuned on cross-attention (CA) and feedforward network (FFN) layers with full-parameter fine-tuning. While both settings show similar performance, it severely overfit and generate some visual artifacts with fabric, as shown in Fig. 7. In contrast, our CA and FFN fine-tuning mitigates overfitting, preserves diversity, and reduces computational cost.

Scale-wise weighted tuning ablation. In our default set-

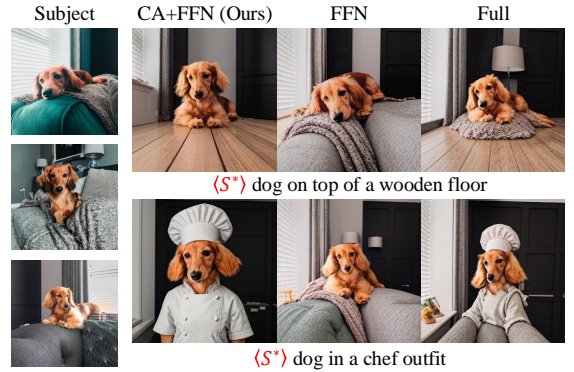


Figure 7. Qualitative comparison of layer selections for tuning.



Figure 8. Qualitative comparison with scale-wise weighted tuning.

ting, we use $w_{>8} = 0.5$ and set the other weight to 1.0. To evaluate the impact of weight settings, we ablate using a configuration where all weights are set to 1.0. As shown in the third row of Tab. 3 and Fig. 8, scale-wise weighted

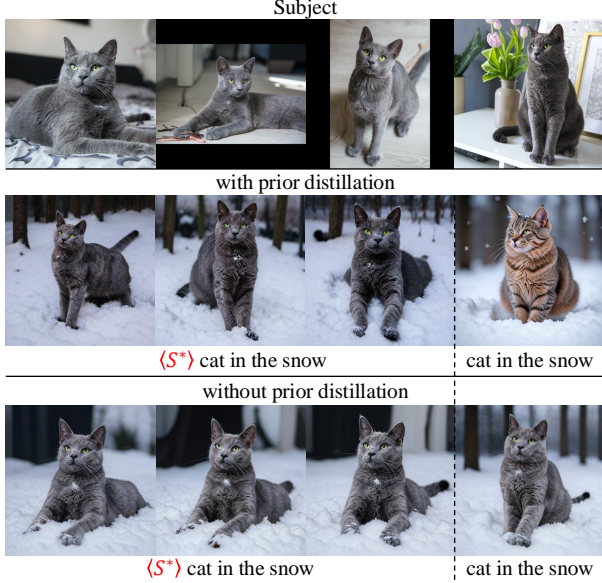


Figure 9. Qualitative comparison with prior distillation.

Model	$I_{dino} \uparrow$	$I_{clip} \uparrow$	$T_{clip} \uparrow$	Time \downarrow
SD3.5-md Full	0.730	0.850	0.205	15s
SD3.5-md LoRA	0.600	0.791	0.275	15s
FLUX-LoRA	0.573	0.793	0.273	55s
Ours	0.786	0.853	0.267	0.5s

Table 4. Quantitative comparison with recent diffusion architecture with DreamBooth [48].

tuning effectively encourages subject fidelity. Although this results in a slight reduction of text alignment, it also preserves prior knowledge, as evidenced by the PRES metrics. This is mainly because scale-wise weighted tuning emphasizes more important coarse-scale token maps inherent in visual autoregressive modeling.

Prior distillation ablation. We compare our model with and without the proposed prior distillation, which aims to mitigate language drift while preserving original priors. As shown in the third row of Tab. 3, prior distillation effectively counteracts language drift and enhances the model’s ability to generate diverse images within prior class. Additionally, DIV metric in Tab. 3 indicates that while prior distillation improves diversity, it comes with a slight reduction in subject fidelity, a trend also observed in Dreambooth [48]. This preservation effect is shown in Fig. 9, where the model with prior distillation exhibits less overfitting to the reference images and generates cats in more diverse poses.

5.6. Additional Analysis

Comparison with baselines in recent diffusion architectures with DreamBooth. Since our base model, Infinity-2B [18], demonstrates strong generative performance compared to Stable Diffusion (SD) 1.4, we ensure a fair comparison by also evaluating DreamBooth [48] on recently re-



Figure 10. Qualitative comparison with recent diffusion architecture with DreamBooth [48].

leased diffusion architectures, including SD 3.5 [10] and FLUX [28, 29], using LoRA [23] plugins. We train all models for the same number of iterations as our approach and evaluate on 5 living subject concepts. As shown in Tab. 4 and Fig. 10, our generated images achieve the highest subject fidelity among the baselines. While SD 3.5-medium-LoRA exhibits better text alignment, our approach maintains higher subject fidelity. These results indicate that VAR-based approach could surpass recent diffusion-based baselines with substantially faster inference speed.

Optimization Time. While our method achieves significantly faster inference than diffusion-based baselines, our optimization time is relatively long, taking approximately 6 hours. For reference, DreamBooth [48] applied on SD 1.4 completes optimization in about 30 minutes. However, larger diffusion-based frameworks with comparable performance to Infinity [18], such as SD 3.5 [10] or FLUX [28, 29], require similar training times to ours. We expect that future work exploring efficient encoder-based tuning methods may further reduce end-to-end duration.

6. Conclusion

In this work, we propose the first subject-driven generation approach using a large-scale visual autoregressive (VAR) model. We introduce selective layer tuning, scale-wise weighted tuning, and prior distillation to address language drift, computational overhead, and reduced diversity. Experiments validate that our method outperforms diffusion-based baselines in subject fidelity, text alignment, and inference speed.

Acknowledgements

This work was supported in part by MSIT/IITP (No. RS-2022-II220680, 2020-0-01821, RS-2019-II190421, RS-2024-00459618, RS-2024-00360227, RS-2024-00437633), MSIT/NRF (No. RS-2024-00357729), KNPA/KIPoT (No. RS-2025-25393280), and SEMES-SKKU collaboration funded by SEMES.

References

- [1] Omri Avrahami, Dani Lischinski, and Ohad Fried. Blended diffusion for text-driven editing of natural images. In *Proceedings of the IEEE/CVF conference on computer vision and pattern recognition*, pages 18208–18218, 2022. 1
- [2] Minwoo Byeon, Beomhee Park, Haecheon Kim, Sungjun Lee, Woonhyuk Baek, and Saehoon Kim. Coyo-700m: Image-text pair dataset. <https://github.com/kakaobrain/coyo-dataset>, 2022. 5
- [3] Mathilde Caron, Hugo Touvron, Ishan Misra, Hervé Jégou, Julien Mairal, Piotr Bojanowski, and Armand Joulin. Emerging properties in self-supervised vision transformers. In *Proceedings of the IEEE/CVF international conference on computer vision*, pages 9650–9660, 2021. 6
- [4] Wenhao Chai, Xun Guo, Gaoang Wang, and Yan Lu. Stable-video: Text-driven consistency-aware diffusion video editing. In *Proceedings of the IEEE/CVF International Conference on Computer Vision*, pages 23040–23050, 2023. 1
- [5] Mark Chen, Alec Radford, Rewon Child, Jeffrey Wu, Heewoo Jun, David Luan, and Ilya Sutskever. Generative pre-training from pixels. In *International conference on machine learning*, pages 1691–1703. PMLR, 2020. 2
- [6] Wenhui Chen, Hexiang Hu, Yandong Li, Nataniel Ruiz, Xuhui Jia, Ming-Wei Chang, and William W Cohen. Subject-driven text-to-image generation via apprenticeship learning. *Advances in Neural Information Processing Systems*, 36:30286–30305, 2023. 2
- [7] Jiwoo Chung, Sangeek Hyun, and Jae-Pil Heo. Style injection in diffusion: A training-free approach for adapting large-scale diffusion models for style transfer. In *Proceedings of the IEEE/CVF conference on computer vision and pattern recognition*, pages 8795–8805, 2024. 1
- [8] Guillaume Couairon, Jakob Verbeek, Holger Schwenk, and Matthieu Cord. Diffedit: Diffusion-based semantic image editing with mask guidance. *arXiv preprint arXiv:2210.11427*, 2022. 1
- [9] Patrick Esser, Robin Rombach, and Bjorn Ommer. Taming transformers for high-resolution image synthesis. In *Proceedings of the IEEE/CVF conference on computer vision and pattern recognition*, pages 12873–12883, 2021. 2
- [10] Patrick Esser, Sumith Kulal, Andreas Blattmann, Rahim Entezari, Jonas Müller, Harry Saini, Yam Levi, Dominik Lorenz, Axel Sauer, Frederic Boesel, et al. Scaling rectified flow transformers for high-resolution image synthesis. In *Forty-first international conference on machine learning*, 2024. 8
- [11] Zhongyi Fan, Zixin Yin, Gang Li, Yibing Zhan, and Heliang Zheng. Dreambooth++: Boosting subject-driven generation via region-level references packing. In *Proceedings of the 32nd ACM International Conference on Multimedia*, pages 11013–11021, 2024. 2
- [12] Haoran Feng, Zehuan Huang, Lin Li, Hairong Lv, and Lu Sheng. Personalize anything for free with diffusion transformer. *arXiv preprint arXiv:2503.12590*, 2025. 14
- [13] Rinon Gal, Yuval Alaluf, Yuval Atzmon, Or Patashnik, Amit Haim Bermano, Gal Chechik, and Daniel Cohen-or. An image is worth one word: Personalizing text-to-image generation using textual inversion. In *The Eleventh International Conference on Learning Representations*. 1, 2, 6
- [14] Rinon Gal, Moab Arar, Yuval Atzmon, Amit H Bermano, Gal Chechik, and Daniel Cohen-Or. Encoder-based domain tuning for fast personalization of text-to-image models. *ACM Transactions on Graphics (TOG)*, 42(4):1–13, 2023. 2
- [15] Mor Geva, Roei Schuster, Jonathan Berant, and Omer Levy. Transformer feed-forward layers are key-value memories. In *Proceedings of the 2021 Conference on Empirical Methods in Natural Language Processing*, pages 5484–5495, 2021. 3
- [16] Mor Geva, Avi Caciularu, Kevin Ro Wang, and Yoav Goldberg. Transformer feed-forward layers build predictions by promoting concepts in the vocabulary space. In *2022 Conference on Empirical Methods in Natural Language Processing, EMNLP 2022*, 2022. 3
- [17] Cusuh Ham, Matthew Fisher, James Hays, Nicholas Kolk, Yuchen Liu, Richard Zhang, and Tobias Hinz. Personalized residuals for concept-driven text-to-image generation. In *Proceedings of the IEEE/CVF Conference on Computer Vision and Pattern Recognition*, pages 8186–8195, 2024. 6
- [18] Jian Han, Jinlai Liu, Yi Jiang, Bin Yan, Yuqi Zhang, Zehuan Yuan, Bingyue Peng, and Xiaobing Liu. Infinity: Scaling bit-wise autoregressive modeling for high-resolution image synthesis. *arXiv preprint arXiv:2412.04431*, 2024. 2, 3, 5, 8
- [19] Amir Hertz, Ron Mokady, Jay Tenenbaum, Kfir Aberman, Yael Pritch, and Daniel Cohen-Or. Prompt-to-prompt image editing with cross attention control. *arXiv preprint arXiv:2208.01626*, 2022. 1
- [20] Amir Hertz, Ron Mokady, Jay Tenenbaum, Kfir Aberman, Yael Pritch, and Daniel Cohen-Or. Prompt-to-prompt image editing with cross-attention control. In *ICLR*, 2023. 1
- [21] Jonathan Ho and Tim Salimans. Classifier-free diffusion guidance. In *NeurIPS 2021 Workshop on Deep Generative Models and Downstream Applications*. 6
- [22] Jonathan Ho, Ajay Jain, and Pieter Abbeel. Denoising diffusion probabilistic models. *Advances in neural information processing systems*, 33:6840–6851, 2020. 5
- [23] Edward J Hu, Yelong Shen, Phillip Wallis, Zeyuan Allen-Zhu, Yuanzhi Li, Shean Wang, Lu Wang, Weizhu Chen, et al. Lora: Low-rank adaptation of large language models. *ICLR*, 1(2):3, 2022. 8, 13
- [24] Xuhui Jia, Yang Zhao, Kelvin CK Chan, Yandong Li, Han Zhang, Boqing Gong, Tingbo Hou, Huisheng Wang, and Yu-Chuan Su. Taming encoder for zero fine-tuning image customization with text-to-image diffusion models. *arXiv preprint arXiv:2304.02642*, 2023. 2
- [25] Dan Kondratyuk, Lijun Yu, Xiuye Gu, José Lezama, Jonathan Huang, Grant Schindler, Rachel Hornung, Vighnesh Birodkar, Jimmy Yan, Ming-Chang Chiu, et al.

Videopoet: a large language model for zero-shot video generation. In *Proceedings of the 41st International Conference on Machine Learning*, pages 25105–25124, 2024. 2

[26] Nupur Kumari, Bingliang Zhang, Richard Zhang, Eli Shechtman, and Jun-Yan Zhu. Multi-concept customization of text-to-image diffusion. In *Proceedings of the IEEE/CVF conference on computer vision and pattern recognition*, pages 1931–1941, 2023. 2, 4, 6

[27] Alina Kuznetsova, Hassan Rom, Neil Alldrin, Jasper Uijlings, Ivan Krasin, Jordi Pont-Tuset, Shahab Kamali, Stefan Popov, Matteo Malluci, Alexander Kolesnikov, et al. The open images dataset v4: Unified image classification, object detection, and visual relationship detection at scale. *International journal of computer vision*, 128(7):1956–1981, 2020. 6

[28] Black Forest Labs. Flux. <https://github.com/black-forest-labs/flux>, 2024. 1, 8, 14

[29] Black Forest Labs, Stephen Batifol, Andreas Blattmann, Frederic Boesel, Saksham Consul, Cyril Diagne, Tim Dockhorn, Jack English, Zion English, Patrick Esser, Sumith Kulal, Kyle Lacey, Yam Levi, Cheng Li, Dominik Lorenz, Jonas Müller, Dustin Podell, Robin Rombach, Harry Saini, Axel Sauer, and Luke Smith. Flux.1 kontext: Flow matching for in-context image generation and editing in latent space, 2025. 8, 14

[30] Doyup Lee, Chiheon Kim, Saehoon Kim, Minsu Cho, and Wook-Shin Han. Autoregressive image generation using residual quantization. In *Proceedings of the IEEE/CVF Conference on Computer Vision and Pattern Recognition*, pages 11523–11532, 2022. 2

[31] Jason Lee, Kyunghyun Cho, and Douwe Kiela. Counteracting language drift via visual grounding. In *Proceedings of the 2019 Conference on Empirical Methods in Natural Language Processing and the 9th International Joint Conference on Natural Language Processing (EMNLP-IJCNLP)*, pages 4385–4395, 2019. 2, 5

[32] Dongxu Li, Junnan Li, and Steven Hoi. Blip-diffusion: Pre-trained subject representation for controllable text-to-image generation and editing. *Advances in Neural Information Processing Systems*, 36:30146–30166, 2023. 2

[33] Senmao Li, Joost van de Weijer, Taihang Hu, Fahad Shahbaz Khan, Qibin Hou, Yaxing Wang, and Jian Yang. Get what you want, not what you don’t: Image content suppression for text-to-image diffusion models. *arXiv preprint arXiv:2402.05375*, 2024. 1

[34] Xiang Li, Kai Qiu, Hao Chen, Jason Kuen, Zhe Lin, Rita Singh, and Bhiksha Raj. Controlvar: Exploring controllable visual autoregressive modeling. *arXiv preprint arXiv:2406.09750*, 2024. 2

[35] Yijun Li, Richard Zhang, Jingwan Lu, and Eli Shechtman. Few-shot image generation with elastic weight consolidation. *arXiv preprint arXiv:2012.02780*, 2020. 2, 4

[36] Zongming Li, Tianheng Cheng, Shoufa Chen, Peize Sun, Haocheng Shen, Longjin Ran, Xiaoxin Chen, Wenyu Liu, and Xinggang Wang. Controlar: Controllable image generation with autoregressive models. *arXiv preprint arXiv:2410.02705*, 2024. 2

[37] Ilya Loshchilov and Frank Hutter. Decoupled weight decay regularization. In *International Conference on Learning Representations*. 6

[38] Yuchen Lu, Soumye Singhal, Florian Strub, Aaron Courville, and Olivier Pietquin. Counteracting language drift with seeded iterated learning. In *International Conference on Machine Learning*, pages 6437–6447. PMLR, 2020. 2, 5

[39] Jiteng Mu, Nuno Vasconcelos, and Xiaolong Wang. Editar: Unified conditional generation with autoregressive models. *arXiv preprint arXiv:2501.04699*, 2025. 2

[40] Jisu Nam, Heesu Kim, DongJae Lee, Siyoon Jin, Seungryong Kim, and Seunggyu Chang. Dreammatcher: appearance matching self-attention for semantically-consistent text-to-image personalization. In *Proceedings of the IEEE/CVF Conference on Computer Vision and Pattern Recognition*, pages 8100–8110, 2024. 1, 6

[41] William Peebles and Saining Xie. Scalable diffusion models with transformers. In *Proceedings of the IEEE/CVF international conference on computer vision*, pages 4195–4205, 2023. 1

[42] Yuang Peng, Yuxin Cui, Haomiao Tang, Zekun Qi, Runpei Dong, Jing Bai, Chunrui Han, Zheng Ge, Xiangyu Zhang, and Shu-Tao Xia. Dreambench++: A human-aligned benchmark for personalized image generation. In *The Thirteenth International Conference on Learning Representations*. 13

[43] Alec Radford, Jong Wook Kim, Chris Hallacy, Aditya Ramesh, Gabriel Goh, Sandhini Agarwal, Girish Sastry, Amanda Askell, Pamela Mishkin, Jack Clark, et al. Learning transferable visual models from natural language supervision. In *International conference on machine learning*, pages 8748–8763. PMLR, 2021. 6

[44] Aditya Ramesh, Prafulla Dhariwal, Alex Nichol, Casey Chu, and Mark Chen. Hierarchical text-conditional image generation with clip latents. *arXiv preprint arXiv:2204.06125*, 1(2):3, 2022. 1

[45] Ali Razavi, Aaron Van den Oord, and Oriol Vinyals. Generating diverse high-fidelity images with vq-vae-2. *Advances in neural information processing systems*, 32, 2019. 2

[46] Scott Reed, Aäron Oord, Nal Kalchbrenner, Sergio Gómez Colmenarejo, Ziyu Wang, Yutian Chen, Dan Belov, and Nando Freitas. Parallel multiscale autoregressive density estimation. In *International conference on machine learning*, pages 2912–2921. PMLR, 2017. 2

[47] Robin Rombach, Andreas Blattmann, Dominik Lorenz, Patrick Esser, and Björn Ommer. High-resolution image synthesis with latent diffusion models. In *Proceedings of the IEEE/CVF conference on computer vision and pattern recognition*, pages 10684–10695, 2022. 1, 5, 6

[48] Nataniel Ruiz, Yuanzhen Li, Varun Jampani, Yael Pritch, Michael Rubinstein, and Kfir Aberman. Dreambooth: Fine tuning text-to-image diffusion models for subject-driven generation. In *Proceedings of the IEEE/CVF conference on computer vision and pattern recognition*, pages 22500–22510, 2023. 1, 2, 4, 5, 6, 8, 13, 14

[49] Nataniel Ruiz, Yuanzhen Li, Varun Jampani, Wei Wei, Tingbo Hou, Yael Pritch, Neal Wadhwa, Michael Rubinstein, and Kfir Aberman. Hyperdreambooth: Hypernetworks for

fast personalization of text-to-image models. In *Proceedings of the IEEE/CVF conference on computer vision and pattern recognition*, pages 6527–6536, 2024. 6

[50] Tim Salimans, Andrej Karpathy, Xi Chen, and Diederik P Kingma. Pixelcnn++: Improving the pixelcnn with discretized logistic mixture likelihood and other modifications. In *International Conference on Learning Representations*, 2017. 3

[51] Christoph Schuhmann, Robert Kaczmarczyk, Aran Komatsu, Aarush Katta, Richard Vencu, Romain Beaumont, Jenia Jitsev, Theo Coombes, and Clayton Mullis. Laion-400m: Open dataset of clip-filtered 400 million image-text pairs. In *NeurIPS Workshop Datacentric AI*, number FZJ-2022-00923. Jülich Supercomputing Center, 2021. 5

[52] Jing Shi, Wei Xiong, Zhe Lin, and Hyun Joon Jung. Instant-booth: Personalized text-to-image generation without test-time finetuning. In *Proceedings of the IEEE/CVF conference on computer vision and pattern recognition*, pages 8543–8552, 2024. 2

[53] Yujun Shi, Chuhui Xue, Jun Hao Liew, Jiachun Pan, Han-shu Yan, Wenqing Zhang, Vincent YF Tan, and Song Bai. Dragdiffusion: Harnessing diffusion models for interactive point-based image editing. pages 8839–8849, 2024. 1

[54] Jascha Sohl-Dickstein, Eric Weiss, Niru Maheswaranathan, and Surya Ganguli. Deep unsupervised learning using nonequilibrium thermodynamics. In *International conference on machine learning*, pages 2256–2265. pmlr, 2015. 5

[55] Jiaming Song, Chenlin Meng, and Stefano Ermon. Denoising diffusion implicit models. In *International Conference on Learning Representations*. 2

[56] Peize Sun, Yi Jiang, Shoufa Chen, Shilong Zhang, Bingyue Peng, Ping Luo, and Zehuan Yuan. Autoregressive model beats diffusion: Llama for scalable image generation. *arXiv preprint arXiv:2406.06525*, 2024. 2

[57] Chameleon Team. Chameleon: Mixed-modal early-fusion foundation models. *arXiv preprint arXiv:2405.09818*, 2024. 2

[58] Keyu Tian, Yi Jiang, Zehuan Yuan, Bingyue Peng, and Liwei Wang. Visual autoregressive modeling: Scalable image generation via next-scale prediction. *Advances in neural information processing systems*, 37:84839–84865, 2025. 2, 3, 13

[59] Aaron Van den Oord, Nal Kalchbrenner, Lasse Espeholt, Oriol Vinyals, Alex Graves, et al. Conditional image generation with pixelcnn decoders. *Advances in neural information processing systems*, 29, 2016. 2, 3

[60] Aäron Van Den Oord, Nal Kalchbrenner, and Koray Kavukcuoglu. Pixel recurrent neural networks. In *International conference on machine learning*, pages 1747–1756. PMLR, 2016. 3

[61] Aaron Van Den Oord, Oriol Vinyals, et al. Neural discrete representation learning. *Advances in neural information processing systems*, 30, 2017. 2

[62] Patrick von Platen, Suraj Patil, Anton Lozhkov, Pedro Cuenca, Nathan Lambert, Kashif Rasul, Mishig Davaadorj, Dhruv Nair, Sayak Paul, William Berman, Yiyi Xu, Steven Liu, and Thomas Wolf. Diffusers: State-of-the-art diffusion models. <https://github.com/huggingface/diffusers>, 2022. 6

[63] Xinlong Wang, Xiaosong Zhang, Zhengxiong Luo, Quan Sun, Yufeng Cui, Jinsheng Wang, Fan Zhang, Yueze Wang, Zhen Li, Qiying Yu, et al. Emu3: Next-token prediction is all you need. *arXiv preprint arXiv:2409.18869*, 2024. 2

[64] Yuqing Wang, Tianwei Xiong, Daquan Zhou, Zhijie Lin, Yang Zhao, Bingyi Kang, Jiashi Feng, and Xihui Liu. Loong: Generating minute-level long videos with autoregressive language models. *CoRR*, 2024. 2

[65] Yuxiang Wei, Yabo Zhang, Zhilong Ji, Jinfeng Bai, Lei Zhang, and Wangmeng Zuo. Elite: Encoding visual concepts into textual embeddings for customized text-to-image generation. In *Proceedings of the IEEE/CVF International Conference on Computer Vision*, pages 15943–15953, 2023. 2, 6

[66] Guangxuan Xiao, Tianwei Yin, William T Freeman, Frédo Durand, and Song Han. Fastcomposer: Tuning-free multi-subject image generation with localized attention. *International Journal of Computer Vision*, pages 1–20, 2024. 2

[67] Jiazheng Xu, Xiao Liu, Yuchen Wu, Yuxuan Tong, Qinkai Li, Ming Ding, Jie Tang, and Yuxiao Dong. Imageward: Learning and evaluating human preferences for text-to-image generation. *Advances in Neural Information Processing Systems*, 36, 2024. 1

[68] Ziyu Yao, Jialin Li, Yifeng Zhou, Yong Liu, Xi Jiang, Chengjie Wang, Feng Zheng, Yuexian Zou, and Lei Li. Car: Controllable autoregressive modeling for visual generation. *arXiv preprint arXiv:2410.04671*, 2024. 2

[69] Ahmet Burak Yildirim, Vedat Baday, Erkut Erdem, Aykut Erdem, and Aysegul Dundar. Inst-inpaint: Instructing to remove objects with diffusion models. *arXiv preprint arXiv:2304.03246*, 2023. 1

[70] Jiahui Yu, Xin Li, Jing Yu Koh, Han Zhang, Ruoming Pang, James Qin, Alexander Ku, Yuanzhong Xu, Jason Baldridge, and Yonghui Wu. Vector-quantized image modeling with improved vqgan. In *International Conference on Learning Representations*. 2

[71] Jiahui Yu, Yuanzhong Xu, Jing Yu Koh, Thang Luong, Gunnar Baid, Zirui Wang, Vijay Vasudevan, Alexander Ku, Yinfei Yang, Burcu Karagol Ayan, et al. Scaling autoregressive models for content-rich text-to-image generation. *Trans. Mach. Learn. Res.*, 2022. 2

[72] Lijun Yu, José Lezama, Nitesh B Gundavarapu, Luca Verasari, Kihyuk Sohn, David Minnen, Yong Cheng, Vighnesh Birodkar, Agrim Gupta, Xiuye Gu, et al. Language model beats diffusion–tokenizer is key to visual generation. *arXiv preprint arXiv:2310.05737*, 2023. 2, 3

[73] Richard Zhang, Phillip Isola, Alexei A Efros, Eli Shechtman, and Oliver Wang. The unreasonable effectiveness of deep features as a perceptual metric. In *Proceedings of the IEEE conference on computer vision and pattern recognition*, pages 586–595, 2018. 6

[74] Yue Zhao, Yuanjun Xiong, and Philipp Krähenbühl. Image and video tokenization with binary spherical quantization. *arXiv preprint arXiv:2406.07548*, 2024. 2, 3

[75] Tianyi Zheng, Cong Geng, Peng-Tao Jiang, Ben Wan, Hao Zhang, Jinwei Chen, Jia Wang, and Bo Li. Non-uniform

timestep sampling: Towards faster diffusion model training.
In *Proceedings of the 32nd ACM International Conference on Multimedia*, pages 7036–7045, 2024. [4](#)

[76] Tianyi Zheng, Peng-Tao Jiang, Ben Wan, Hao Zhang, Jinwei Chen, Jia Wang, and Bo Li. Beta-tuned timestep diffusion model. In *European Conference on Computer Vision*, pages 114–130. Springer, 2024. [4](#)

Supplementary Material

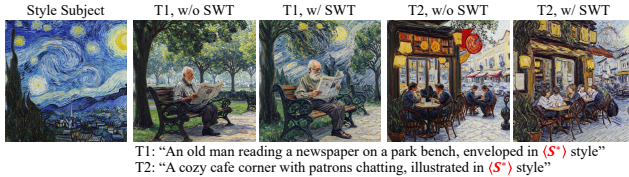


Figure 11. Qualitative comparison demonstrating the effectiveness of Scale-wise Weighted Tuning (SWT) for style personalization.

A. Additional Ablations

A.1. Scale-wise Weighted Tuning for Style Personalization

Unlike diffusion models, where later timesteps capture fine, high-frequency details, our analysis indicates that later scales of large-scale pretrained VAR models contribute minimally to output variation. Consequently, our proposed Scale-wise Weighted Tuning (SWT) strategy deemphasizes these scales, improving robustness in style personalization tasks, particularly for capturing high-frequency details.

To validate SWT effectiveness, we fine-tune on eight distinct style concepts from DreamBench++ [42], each with nine text prompts, for 100 iterations per style. We generate eight outputs per pair and present representative qualitative comparisons in Fig. 11. As shown in Fig. 11, SWT achieves clearer stylistic expressions, such as distinct swirls and brushstrokes.

A.2. Prior Distillation vs. Prior Preservation Loss

We further compare our Prior Distillation (PD) method against the Prior Preservation Loss (PPL) approach [48]. For integrating PPL into VAR [58], we replace the original MSE objective with cross-entropy objective, using 100 class-specific images generated with the Infinity-2B checkpoint.

Quantitative results in Tab. 5 and qualitative results in Fig. 12 demonstrate comparable performance between PD and PPL across various metrics. Notably, PD eliminates the requirement for same-class dataset collection, substantially reducing the preparation time and computational overhead.

A.3. Selective Layer Tuning with LoRA

We evaluate Selective Layer Tuning (SLT) combined with Prior Distillation (PD) against the popular LoRA method [23]. Specifically, we apply LoRA across all VAR layers at multiple ranks (4 and 16) without employing SLT or PD, to isolate their contributions. As shown in Tab. 6,



Figure 12. Qualitative comparison between our Prior Distillation (PD) and Prior Preservation Loss (PPL).

Variant	$I_{dino} \uparrow$	$I_{clip} \uparrow$	$T_{clip} \uparrow$	$PRES \downarrow$	$DIV \uparrow$
Ours w/ PD	0.786	0.853	0.267	0.709	0.272
Ours w/ PPL	0.653	0.822	0.265	0.608	0.378

Table 5. Quantitative comparison between our Prior Distillation (PD) and Prior Preservation Loss (PPL).

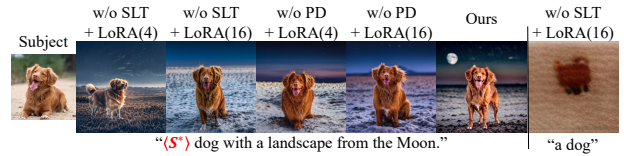


Figure 13. Qualitative comparison of LoRA adaptation versus our SLT + PD approach.

Base	Adapter	$I_{dino} \uparrow$	$I_{clip} \uparrow$	$T_{clip} \uparrow$	$PRES \downarrow$	$DIV \uparrow$
w/o SLT	+ LoRA(4)	0.653	0.822	0.265	0.608	0.378
	+ LoRA(16)	0.770	0.852	0.264	0.383	0.351
w/o PD	+ LoRA(4)	0.753	0.852	0.265	0.676	0.376
	+ LoRA(16)	0.775	0.854	0.265	0.781	0.373
Ours (w/ SLT, PD)		0.786	0.853	0.267	0.709	0.272

Table 6. Quantitative comparison with LoRA.

LoRA without SLT or PD results in unstable fine-tuning, causing visual artifacts or failing to accurately capture subject concepts.

The qualitative results in Fig. 13 further confirm that our combined approach (SLT + PD) stabilizes personalization and preserves subject identity, validating their critical role in achieving robust VAR personalization.

B. User Study Details

We conduct a user study with 20 participants to evaluate personalization effectiveness. Participants compare outputs from our method against baselines, focusing on subject fidelity and prompt alignment, following the evaluation pro-

Please select the best image among the generated images (a, b, c) according to the evaluation criteria.

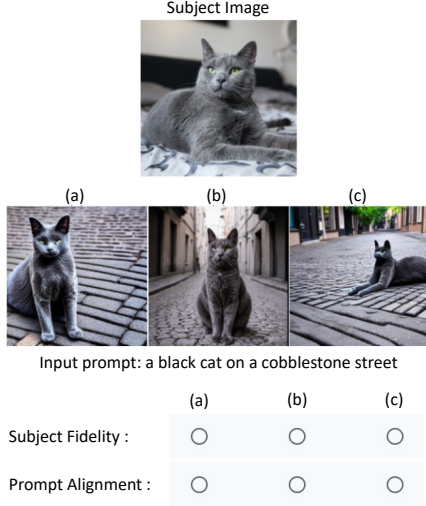


Figure 14. User study interface for evaluating personalization quality.



Figure 15. Qualitative comparison to Personalize Anything (PA) [12].

tocol from DreamBooth [48]. The user interface is shown in Fig. 14.

C. Additional Qualitative Comparisons

C.1. Comparison with FLUX-based Method

We further compare our VAR-based approach with Personalize Anything (PA) [12], which is based on the FLUX framework [28, 29]. As illustrated in Fig. 15, PA [12] struggles to generate dynamic poses from the subject image, whereas our approach successfully synthesizes diverse and dynamic poses, highlighting the efficacy of our VAR-based personalization.

C.2. Comparison with Diffusion-based Methods

Additional qualitative comparisons against diffusion-based baselines are provided in Fig. 16. These examples clearly demonstrate our method’s ability to better preserve subject identity, accurately capturing crucial attributes such as color and shape. Furthermore, our method achieves notably improved alignment with the provided prompts.

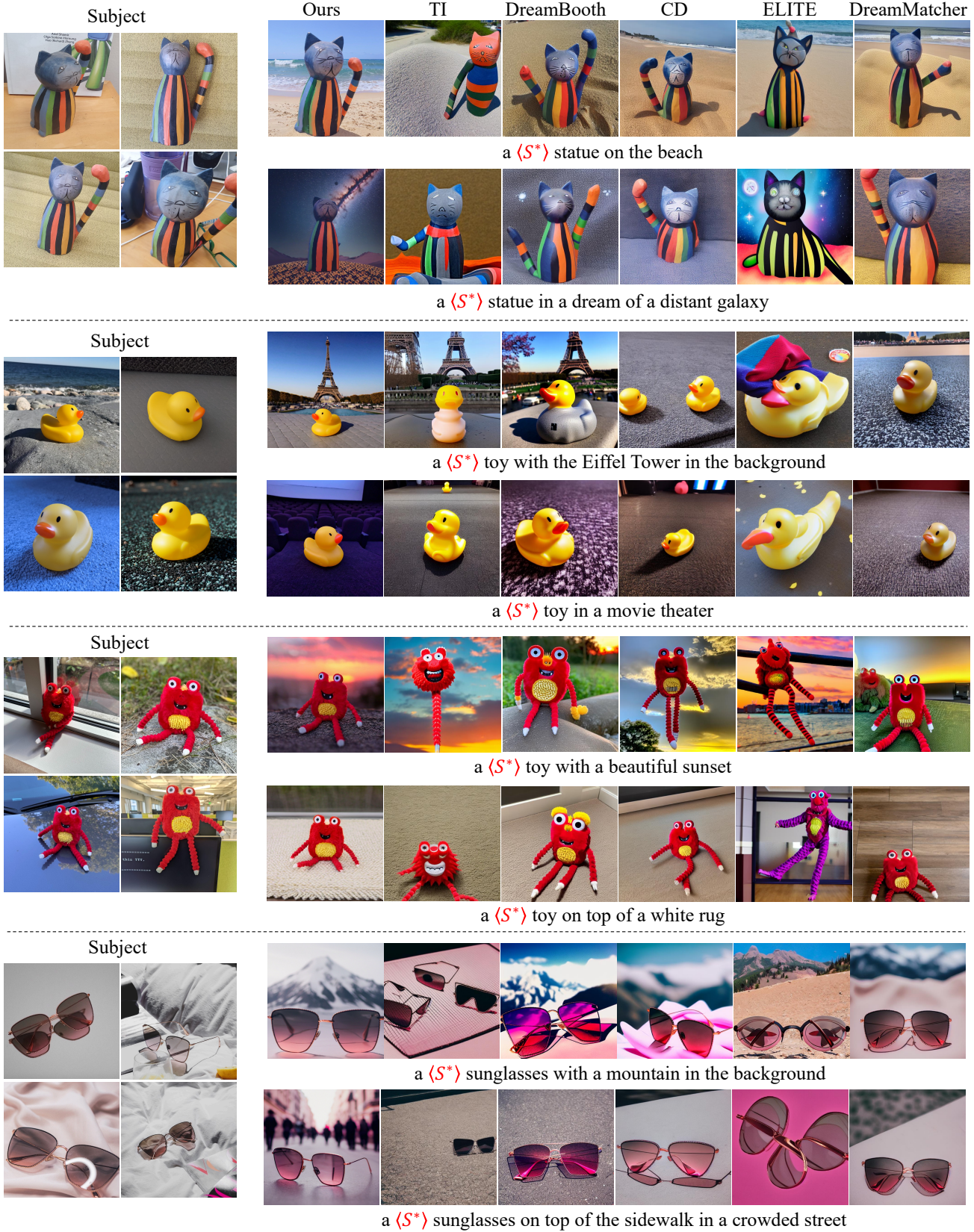


Figure 16. Extended qualitative comparisons to diffusion-based baselines.